Biochemical Pharmacology, Vol. 57, pp. 97–110, 1999.

ISSN 0006-2952/99/$–see front matter
PII S0006-2952(98)00289-5

Induction of Human Breast Cancer Cell Apoptosis from G_2/M Preceded by Stimulation into the Cell Cycle by Z-1,1-Dichloro-2,3-diphenylcyclopropane

Raghavan Balachandran, Ernst ter Haar,*† Jack C. Yalowich,‡‖ Manda J. Welsh,* Stephen G. Grant*§‖ and Billy W. Day*‖¶***

*Department of Environmental & Occupational Health, ¶Department of Pharmaceutical Sciences, ‡Department of Pharmacology, §Department of Obstetrics, Gynecology and Reproductive Sciences, the Magee-Womens Research Institute, and the ‖University of Pittsburgh Cancer Institute, University of Pittsburgh, Pittsburgh, PA 15238, U.S.A.

ABSTRACT. We have shown previously that Z-1,1-dichloro-2,3-diphenylcyclopropane (a.k.a. Analog II, A_{II}) inhibits human breast cancer cell proliferation regardless of estrogen receptor status or estrogen sensitivity, and that its cellular targets include microtubules. In the present study, we investigated the apoptosis-inducing effects of A_{II}. MCF-7, MCF-7/LY2, and MDA-MB-231 cells all showed nuclear fragmentation in response to 100 μM A_{II} when stained with Hoechst 33342 and examined by fluorescence microscopy. Pulsed field gel electrophoretic analysis showed that each of the cell lines also developed specific high molecular weight DNA fragments: a low level of 1–2 Mb fragments appeared after 6 hr, while 30–50 kb fragments accumulated subsequently. At 24 hr of drug exposure, the majority of cells became nonadherent, and the 30–50 kb fragments were restricted to detached MCF-7 and MDA-MB-231 cells. Both adherent and detached MCF-7/LY2 cells exhibited these fragments. A previous study by single-color (propidium) flow cytometry demonstrated that A_{II} blocks MDA-MB-231 cells in G_2/M of the cell cycle. More refined analyses in the present study showed this same result for MDA-MB-231 cells, but MCF-7 and MCF-7/LY2 cells did not reveal apparent drug-induced cell cycle block. A_{II} demonstrated growth inhibitory, cell cycle-perturbing, and hypodiploidy-inducing activity against other human breast carcinoma lines, i.e. BT-20, CAMA-1, and SKBR-3, but no such actions in the non-tumorigenic, "normal" human breast epithelial line MCF-10A. Bromodeoxyuridine labeling and two-color flow cytometric analysis, however, suggested that A_{II} caused stimulation into S phase, and that G_2/M was the phase of the cell cycle from which cells apoptosed. A_{II} caused cell rounding, detachment from the growth matrix, and nuclear shrinkage and fragmentation in parallel with biochemical changes. Cycloheximide inhibited A_{II}-induced cell death, indicating that its toxicity requires *de novo* protein synthesis. BIOCHEM PHARMACOL **57**;1:97–110, 1999.

KEY WORDS. Analog II; flow cytometry; pulsed field gel electrophoresis; bromodeoxyuridine; cycloheximide; Hoechst 33342

A_{II}†† (a.k.a. Analog II) (Fig. 1) is a known anti-breast tumor agent with low toxicity (LD_{50} of >3000 mg/kg) in rodent models [1–4]. A_{II} originally was suggested to be a competitive inhibitor of estrogen binding to the high affinity–low capacity type I estrogen binding site (ER), i.e. an antiestrogen, even though it has long been known to have little to no affinity for the ER [4, 5]. We have shown recently that A_{II} has antiproliferative activity against human breast cancer cells in culture regardless of their ER status, that the early effects of low concentrations of A_{II} appear to be primarily cytostatic, and that the agent, even if metabolically activated, is not mutagenic in bacteria [6], in agreement with the results of others in eukaryotic cells [7]. A_{II} has rapid effects on the microtubule network of cells, and directly inhibits the assembly of α/β-tubulin heterodimers into microtubules *in vitro* [8].

Our most recent study suggested that A_{II} causes hypodiploidy, one indication of apoptosis, subsequent to G_2/M accumulation in the MDA-MB-231 human breast carcinoma cell line [8]. The role of apoptosis in cancer therapy has gained widespread attention [9, 10]. Although apoptosis is a normal process in development and morphogenesis, its pathways are altered or lost in some cancer cells. Many

† Present address: Department of Cell Biology and Center for Blood Research, Harvard Medical School, Boston, MA 02115.

** Corresponding author: Billy W. Day, Ph.D., Departments of Environmental & Occupational Health and of Pharmaceutical Sciences, University of Pittsburgh, 260 Kappa Drive, Pittsburgh, PA 15238. Tel. (412) 967-6502; FAX (412) 624-1020; E-mail: bday+@pitt.edu.

†† *Abbreviations:* A_{II}, Z-1,1-dichloro-2,3-diphenylcyclopropane (a.k.a. Analog II); BrdU, 5-bromo-2′-deoxyuridine; CHX, cycloheximide; ER, estrogen receptor; FBS, fetal bovine serum; FITC, fluorescein-5-isothiocyanate; HBSS, Hanks' balanced salt solution; HMW, high molecular weight; PFGE, pulsed field gel electrophoresis; and PI, propidium iodide.

Received 23 April 1998; accepted 4 August 1998.

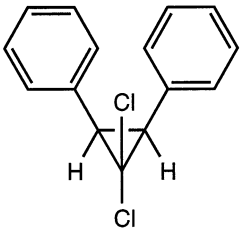

FIG. 1. Structure of Z-1,1-dichloro-2,3-diphenylcyclopropane (A_{II}).

antitumor drugs reduce the proliferative potential of neoplastic cells by disrupting their passage through the cell cycle [11–13], thereby activating a cascade of signals to initiate the cell death program [14, 15]. Apoptosis is characterized by a number of changes in the nucleus, chromatin, and cell membrane. In cells of hematopoietic origin or certain epithelial cells (e.g. somatic cells in the ovary), internucleosomal DNA fragmentation is the hallmark of apoptosis [16, 17]. Yet, in many malignant cells, such low molecular weight DNA fragments do not appear and, if they do, are more likely a result of necrotic mechanisms [18]. Changes in nuclear structure and the presence of HMW DNA fragments during apoptotic cell death have been reported in a variety of human epithelial cancer cell types [19, 20]. The integrity of cellular chromatin is often lost when epithelial cell types are induced to detach from monolayer cultures by a variety of biological and physiological conditions [17, 19, 20]. Field inversion and PFGE analyses have revealed the appearance of large, regularly sized DNA fragments (30–50 and/or 400–600 kb) in transformed epithelial cells detached from their growth matrix [19]. In some cell lines, apoptosis is characterized by both high and low molecular weight DNA fragmentation. Apparently, when both types of fragments appear, the larger precede the smaller. The HMW fragments can appear within minutes of drug treatment and are one of the earliest detectable events in the onset of apoptosis [21, 22].

While some neoplastic cells are termed "apoptosis proficient" (i.e. they undergo internucleosomal DNA fragmentation), others are deficient in this portion of the apoptotic pathway. Neoplastic transformation has apparently conferred resistance to, or loss of, the ability to perform this low molecular weight DNA fragmentation in some breast cancer cells [23]. Under certain conditions where attachment to the growth matrix plays an important role in cell viability, however, human breast cancer epithelial cells will exhibit low molecular weight fragmentation. For example, MCF-7 cells implanted into nude mice undergo internucleosomal DNA fragmentation following estrogen ablation [24]. Also, others have shown that the growth matrix-detached fraction of MDA-MB-468 cells treated *in vitro* with 5-fluorouracil, epidermal growth factor, or paclitaxel will form internucleosomal DNA fragments [25–27]. This programmed cell death in response to the loss of cell-to-cell and/or cell-to-matrix communication has been termed anoikis, or "loss of home" [17].

In this investigation, experiments were performed to study the mode of death caused by A_{II} in human breast cancer cells. We found that A_{II} specifically activated cellular mechanisms for apoptosis, causing the morphological characteristics of this process as well as HMW DNA fragmentation and induction of a hypodiploid cell population in human breast cancer cells of differing ER status, estrogen responsiveness, and drug sensitivity. This action was shown to be cell cycle-dependent, to require *de novo* protein synthesis, and was dependent upon the adherence status of the cell. A_{II} showed these activities against a broad range of human breast carcinoma cell lines, but not against a non-tumorigenic, "normal" human breast cell line. Coupled with its known antitumor action and extremely low lethality in rodent models, the sum of our data argues that A_{II} represents a new class of multifunctional agents that show promise for the treatment of human breast cancer.

MATERIALS AND METHODS

Materials

A_{II} was synthesized as described previously [6, 28, 29]. It was dissolved in DMSO, and control samples contained vehicle equivalent to that in drug-treated cultures. MCF-7 cells (28th passage) were a gift from Dr. Marc Lippman (Vincent T. Lombardi Cancer Center), as was the antiestrogen-resistant MCF-7/LY2 line. MCF-10A cells were obtained from the Michigan Cancer Foundation. All other cell lines were purchased from the American Type Culture Collection. Phenol red-free IMEM culture medium was purchased from Biofluids, and FBS from Hyclone Laboratories, Inc. RPMI 1640 culture medium, Ca^{2+}- and Mg^{2+}-free HBSS, glutamine, Trypan blue dye, the 123 bp DNA marker ladder standard and trypsin were obtained from Gibco-BRL Life Technologies, Inc. InCert and LE agarose were purchased from the FMC Corp. BioProducts, while Pulsed Field Certified Agarose was obtained from Bio-Rad Laboratories. Proteinase K was obtained from Boehringer Mannheim. *Saccharomyces cerevisiae* chromosomes and lambda phage ladders were from New England Biolabs. Giemsa stains were from Fisher Scientific. Normal rabbit serum, monoclonal mouse anti-5-bromo-2′-deoxyuridine (BrdU) (M744), and polyclonal FITC-conjugated rabbit antimouse (F313) antibodies were obtained from the Dako Corp. All other chemicals and materials were purchased from the Sigma Chemical Co.

Cell Culture [6, 8]

Cells were maintained in RPMI-1640 with phenol red containing 10% FBS. During drug treatment, cells in-log-phase growth were plated in at least triplicate in 60-mm dishes and grown in IMEM without phenol red containing 2.5% serum. Drug treatment was initiated 48–72 hr after replating. Viable cell numbers and surviving fractions were determined after combining floating cells with trypsinized

attached cells microscopically using Trypan blue exclusion on a hemacytometer.

Detection of Nuclear Fragmentation

Cells were grown on glass cover slips and exposed to drug or vehicle for the time periods listed in the text. Adherent and non-adherent (the latter collected and concentrated on a microscope slide with a CytoSpin apparatus) cells were fixed separately in 1% buffered formalin for 10 min, washed with HBSS, and resuspended in 20 μg/mL of Hoechst 33342 in HBSS for 15 min at room temperature. Nuclei were visualized using a Nikon Microphot-PX photomicroscope with a Xe lamp/epifluorescence attachment and photographed using Kodak ASA film.

Cell Morphological Analyses

These analyses were performed by light microscopy on cells grown, treated, and collected as above. The cells were fixed in 4% buffered formalin, and were stained with May-Grunwald for 10 min and then with 19:1 Wright-Giemsa for 20 min.

Cell Cycle Analysis

Cellular DNA content was quantified by flow cytometric determination of PI intercalated into DNA of intact, fixed cells. Drug- or vehicle-treated cells (1×10^6) were collected, resuspended in HBSS, and fixed in 70% ethanol at −20° for 30 min. Cells were pelleted by centrifugation and then treated with RNase A (100 μg/mL) in 0.9 mL of HBSS at 37° for 30 min, 0.1 mL of PI (1 mg/mL) was added, and the cells were stored in the dark at 4° until analyzed. DNA content was determined on a Becton-Dickinson FACScan flow cytometer equipped with a 488 nm Ar laser by measuring forward and orthogonal light scatter and peak and area red fluorescence. Cell cycle populations were quantified from a standard count of 10,000 cells, using the Lysis II program.

Preparation of Cells for Electrophoretic Analyses

Agarose plugs for electrophoretic analyses were each made with 1×10^6 cells. Total cells were suspended in 10 mM Tris containing 20 mM NaCl and 50 mM EDTA, pH 7.2, equilibrated at 50°. An equal volume of InCert agarose was added, and plugs were formed in LKB Bromma molds. After solidification at 4°, plugs were incubated overnight at 50° in 4.8 mM sodium deoxycholate, 42 mM sodium dodecylsulfate, 10 mM EDTA, pH 8.0, containing 500 μg/mL of Proteinase K, and then were washed four times with 50 mL of 20 mM Tris, 50 mM EDTA, pH 8.0.

Static Field Gel Electrophoresis

Analysis for internucleosomal ladders was performed on cell plugs loaded into slots of a 1.5% agarose gel and sealed in with molten agarose. Electrophoresis was performed in TBE buffer (89 mM Tris, 50 mM boric acid, 2 mM EDTA) at 75 V constant current for 6 hr. A standard DNA marker ladder (123 bp) was included in each gel. Gels were stained with ethidium bromide (1 μg/mL) and then were visualized by UV transillumination.

PFGE Analysis

PFGE analysis of DNA from cells was performed in TBE buffer at 10° with an LKB Bromma PulsaPhor Electrophoresis unit on cell plugs loaded into slots of 1.5% Pulsed Field Certified Agarose and sealed in with molten agarose. Electrophoresis parameters optimized for 30–70 kb fragments were 60–100 sec pulses for 40 hr at 180 V (6 V/cm) from an LKB Bromma 2015 PulsaPhor Plus control unit. Marker lanes were loaded with *S. cerevisiae* chromosomes (225–1900 kb) and lambda phage ladders (48.5–1018 kb). After electrophoretic separation, gels were stained with ethidium bromide (1 μg/mL) for 1 hr and then were visualized with a UV transilluminator. Gel images were collected and digitized with a UVP Image-Store 5000 gel data documentation system. Band densities were estimated with the NIH Image (version 1.6) software.

BrdU Labeling of DNA

A modification of the procedures of Dolbeare *et al.* [30] was used, all performed in subdued light. Cells were treated with 10 μM BrdU for 30 min, followed by addition of drug, in complete culture medium. Total cells were collected at 6-hr intervals, washed twice in HBSS, and fixed in 70% ethanol at −20°. The cells were pelleted by centrifugation at 4° and rinsed with cold HBSS. Following gentle vortexing, the pellet was resuspended in 1 mL of 2 N HCl containing 0.2 mg/mL of pepsin and incubated at room temperature for 30 min. The HCl was neutralized with 1 mL of 1 M $Na_2B_4O_7$, and cells were pelleted by centrifugation and resuspended in 200 μL of HBSS. Monoclonal mouse anti-BrdU antibody (100 μL of a 1:27 dilution) was added, and the samples were incubated on ice for 30 min. Then cells were washed in 2 mL of cold HBSS and pelleted by centrifugation. The supernatant was removed to leave a residual volume of 200 μL, and the cell pellet was treated with 100 μL of the $F(ab')_2$ fragment of polyclonal FITC-conjugated rabbit antimouse antibody (1:30 dilution) containing 5% normal rabbit serum for an additional 15 min on ice. Then cells were washed, pelleted by centrifugation, and suspended in 800 μL of HBSS, 100 μL of 1 mg/mL of RNaseA and 100 μL of 1 mg/mL of PI. Two-color flow cytometric analysis was done as described above by simultaneous detection of green and red fluorescence.

Effects of CHX

Triplicate cell samples in six-well plates (5×10^4 cells/well) were preincubated with 18 μM (5 μg/mL) CHX for 12 hr. Preliminary ranging experiments showed that this was the maximum concentration of CHX with no effect on cell viability, but it caused a significant (*ca.* 80%) inhibition of protein synthesis (determined by the Lowry assay of cell lysates). Cells were washed subsequently with HBSS and exposed to 100 μM A_{II} alone or in the presence of 5 μg/mL of CHX. After 4 and 12 hr, the medium was transferred to a centrifuge tube. Attached cells were gently trypsinized, collected, and added to the cells from the medium. An aliquot of the combined cells was then quantified microscopically and examined by PFGE and PI flow cytometry as described above.

RESULTS

A_{II}-Induced Changes in Cellular and Nuclear Morphology

To study the potential apoptosis-inducing effects of A_{II} in human breast carcinoma cells, a drug concentration of 100 μM was chosen. Based on our previous studies, continuous exposure to this level of drug for 24 hr causes massive microtubule perturbation in a significant fraction of cells, full cytostasis, and ultimately reduces cell survival by approximately 50% [6, 8]. Furthermore, 100 μM is a physiologically achievable, subtoxic concentration of the drug [1–4]. The ER negative/estrogen nonresponsive MDA-MB-231 cell line was studied initially for direct comparison to our previous studies [6, 8].

Cells undergoing apoptosis show typical morphological characteristics, including cell shrinkage, condensation of the nucleus, and formation of apoptotic bodies. The effects of A_{II} on cell morphology were examined in adherent cells by Giemsa staining, and adherent and detached cells were examined with the fluorescent chromatin dye Hoechst 33342. Giemsa staining of A_{II}-treated MDA-MB-231 cells showed that remarkable nuclear condensation occurred as early as 4 hr into drug treatment. This process was also associated with changes in cell shape, as they lost their typical, elongated fibroblast-like morphology, becoming rounded with a decreased cytoplasmic space (data not shown). A large portion of the cells stained with Hoechst 33342 had apoptotic bodies and/or irregularly punctate nuclei, characteristic of cells undergoing programmed cell death (Fig. 2). Detached cells showed the highest amount of nuclear fragmentation, which differed distinctly from the nuclear staining pattern found in control mitotic cells. Some of the attached cells also showed nuclear pyknosis, often considered characteristic of necrosis. These pyknotic nuclei-containing cells were shrunken, however, instead of swollen as is expected for cells dying by a necrotic mechanism.

MCF-7 and MCF-7/LY2 cells, each, respectively, ER positive/estrogen responsive and ER positive/antiestrogen resistant, were also examined for A_{II}-induced morphological changes. Along with MDA-MB-231, these cell lines were chosen to represent the range of hormone sensitivity found in human breast tumors. Giemsa staining again showed that nuclear condensation occurred early into drug treatment with these two cell lines. Normal cell morphology (irregular ovoid for MCF-7 and MCF-7/LY2) was lost in a time-dependent manner, and the cells also became rounded in response to the drug (data not shown). Hoechst 33342 staining again showed high amounts of nuclear fragmentation and pyknosis (Fig. 2).

A_{II}-Induced Perturbation of the Cell Cycle

Combined attached and detached cells were analyzed by PI flow cytometry for changes in DNA content and cell cycle distribution for comparison with DNA fragmentation patterns (Fig. 3). As we had seen previously [8], MDA-MB-231 cells showed evidence of accumulation into the G_2/M phase of the cell cycle by 12 hr of treatment. There was no apparent change in the S phase fraction of MDA-MB-231 cell populations, and a slight increase in hyperploid cells. Unlike our previous flow cytometric analyses of A_{II}-treated cells [8], in this work we used a method that allows for close inspection of hypodiploid cell populations—collection of data such that fluorescence intensity (the x-axis) was displayed on a log scale. Using this method, we observed only a 2- to 4-fold increase in hypodiploid MDA-MB-231 cells.

A_{II} treatment of MCF-7 cells caused a slight increase (10–20%) in their G_1 to G_2/M ratio, a 2-fold increase in S-phase cells, a 1.5- to 2-fold decrease in hyperploid cells, and only a 2- to 4-fold increase in hypodiploid cells as compared with controls. It should be noted that the drug-induced increases or decreases in hyperploid populations is proof that a hyperploid population existed (and was not an artifact of the flow cytometry conditions) and that the drug affected its number. In MCF-7/LY2 cells, the drug induced an even more pronounced (2- to 4-fold) increase in the G_1 to G_2/M ratio. There was also a prominent increase (10- to 60-fold) in the hypodiploid population, indicative of minicell formation, i.e. apoptotic bodies, that progressively increased over the 24-hr treatment period. As with the MCF-7 cells, MCF-7/LY2 cells experienced a 2-fold increase in S-phase cells in response to the drug. There was also a marked and progressive decrease in the normally abundant hyperploid population of this cell line.

With each of the three cell lines, 24 hr of exposure to 100 μM A_{II} caused a majority of cells to become nonadherent. Drugs that affect microtubule dynamics almost invariably block cells at the G_2/M phase of the cell cycle [31], and mitotic epithelial cells are more easily detached from cell culture plates (e.g. "mitotic shakeoff" experiments). Yet, the flow cytometry results from analysis of the combined attached and detached cells presented above did not show accumulation into G_2/M for A_{II}-treated MCF-7 or MCF-7/LY2 cells. We suspected that the large amount of

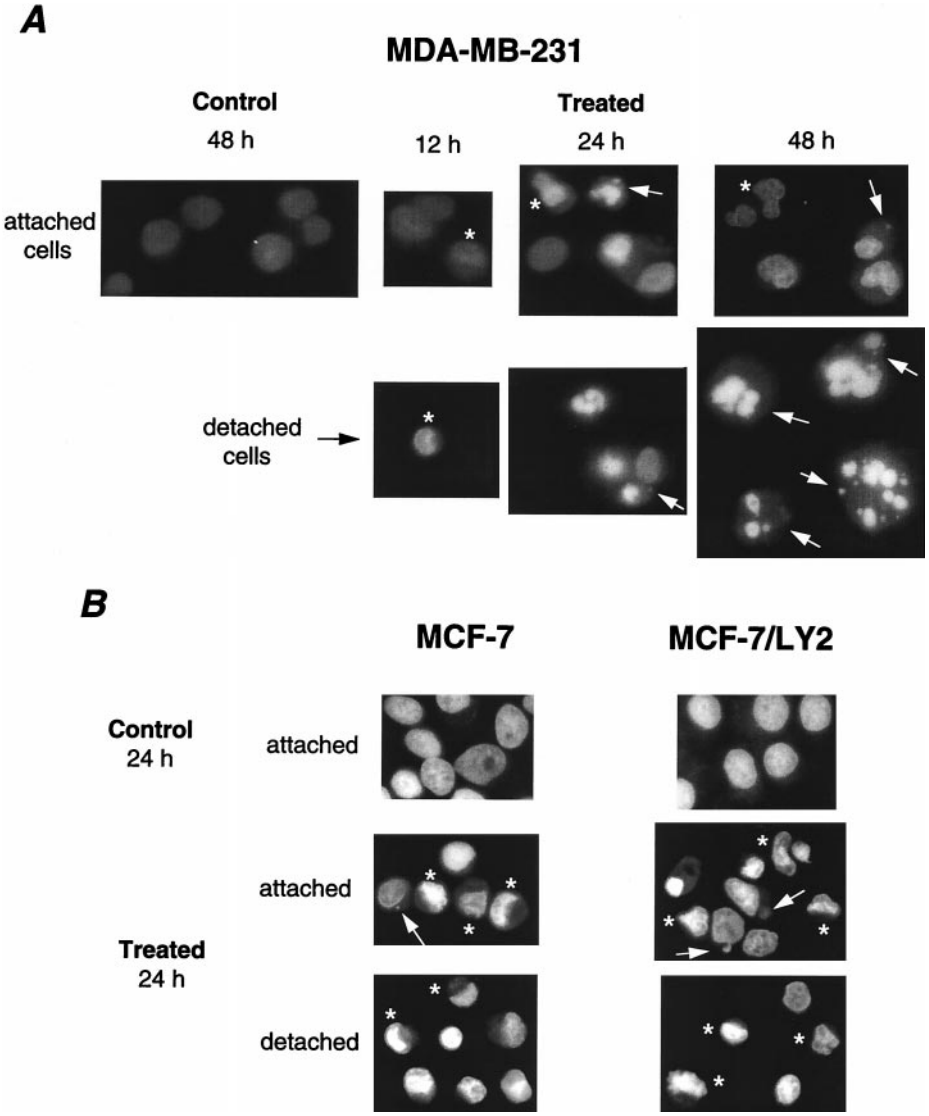

FIG. 2. Examples of the nuclear morphological changes induced by 100 μM A_{II} in (A) MDA-MB-231, and (B) MCF-7 and MCF-7/LY2 cells. Arrows: apoptotic bodies/fragmented nuclei. Asterisks: pyknotic nuclei.

cell detachment that results from A_{II} treatment was a clue that would assist in rectifying this apparent difference between the cell lines examined. Adherent and detached cells were thus collected separately and analyzed by PFGE and PI flow cytometry.

A_{II}-Induced HMW DNA Fragmentation

Drug-treated and vehicle-treated control cells (both floating and attached) were collected at 6-hr intervals during a 24-hr period and analyzed for DNA fragmentation by both static field gel electrophoresis and PFGE. Static field electrophoretic analyses did not reveal internucleosomal DNA fragmentation ("ladders") in these breast cancer cell lines (data not shown), in agreement with many studies [18, 27]. PFGE analysis, on the other hand, showed that A_{II} induced formation of HMW DNA fragments, which were detectable as early as 6 hr (MCF-7/LY2 cells) and evident in all cell lines by 18 hr of drug treatment (Fig. 3). Similar to what we recently reported in these cell lines for two known apoptosis-inducing microtubule perturbing drugs, paclitaxel and discodermolide [32], it was apparent from the PFGE gels that A_{II} treatment caused DNA to be initially cleaved to 1–2 Mb fragments, followed in some cases by cleavage to intermediate fragments of 400–600 kb, and finally in all cases into 30–50 kb fragments. This fragmentation occurred in a time-dependent manner, with increasing amounts of 30–50 kb DNA fragments accumulating and detectable in all three cell lines at the 24-hr time point. Control cells did not show any fragmentation beyond 1–2 Mb.

PFGE experiments showed that the 30–50 kb fragments were restricted to the detached fraction of A_{II}-treated MCF-7 and MDA-MB-231 cells (Fig. 4). In some experiments, both attached and detached A_{II}-treated MCF-7/LY2 cells exhibited these fragments, although they were always more abundant in the detached cells. In other experiments with this cell line, only the detached cells had 30–50 kb HMW DNA fragments. To determine if the cells remaining attached after 24 hr of drug treatment would continue on to

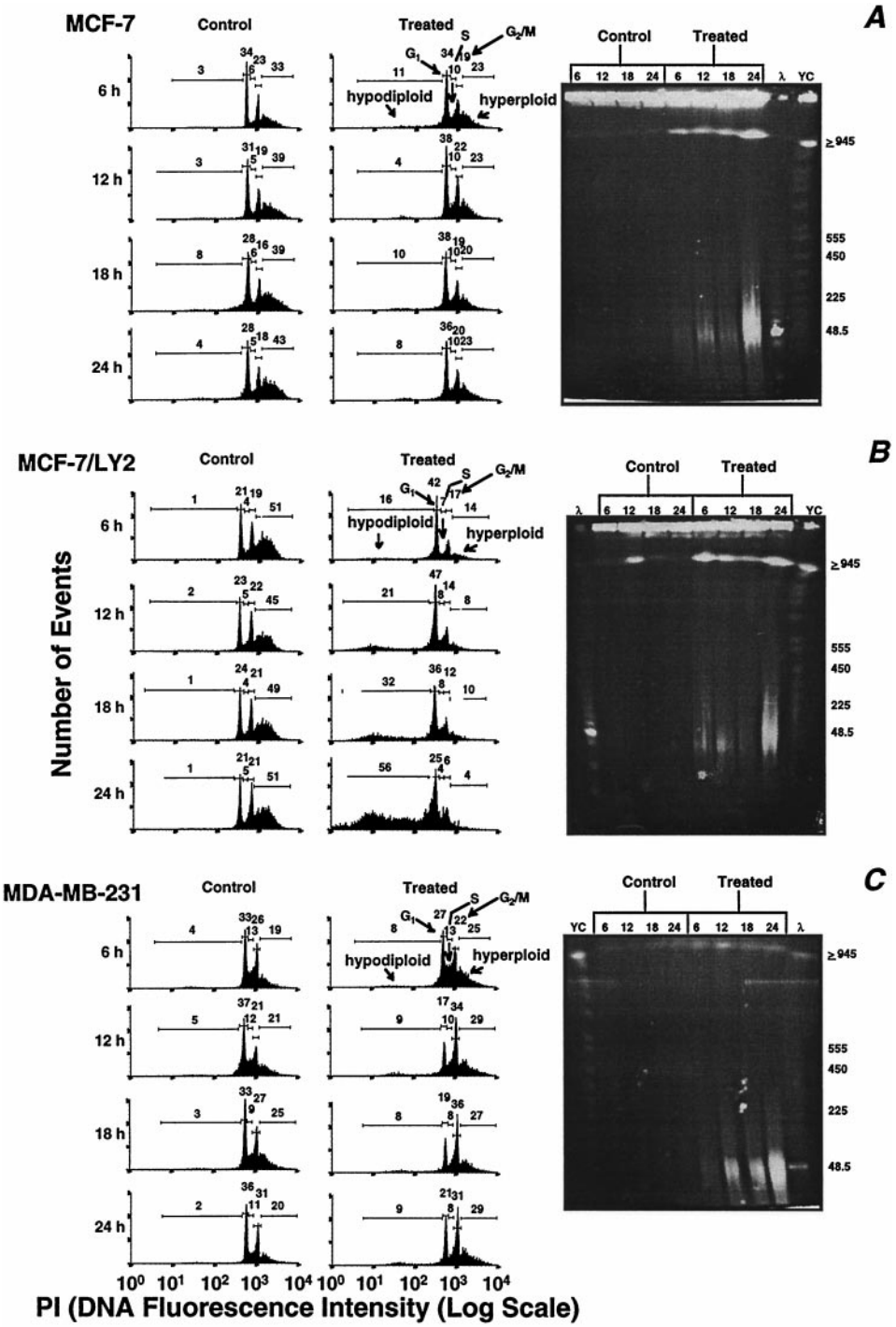

FIG. 3. PI flow cytometric and pulsed field gel electrophoretic analysis of MCF-7 (A), MCF-7/LY2 (B), and MDA-MB-231 (C) human breast cancer cells treated with 100 μM A_{II} for 6–24 hr. Control cells treated for the same time periods with vehicle (DMSO) are shown for comparison. Ethanol-fixed cells were treated with RNase A and PI, and DNA content was determined with a 488 nm Ar laser by measuring forward and orthogonal light scatter and peak and area red fluorescence. Cell cycle populations were quantified from a standard count of 10,000 cells. Numbers above bars in the histograms give the percentage of cells in that region. Note that data were collected so that the histograms are presented with log scale x-axes (fluorescence/event). Pulsed field gel electrophoresis analysis (on a 1.5% agarose gel) of duplicate cultures are shown to the right of the flow profiles. Lanes are labeled with the hours of treatment with vehicle (Control) or drug (Treated). λ, lambda phage markers; YC, *S. cerevisiae* chromosomes.

develop 30–50 kb fragments after drug removal, experiments were performed wherein cells were treated with drug for 24 hr, detached cells were removed (and analyzed by PFGE), and attached cells were grown in fresh, drug-free medium for an additional 24 hr. Both MCF-7/LY2 and MDA-MB-231 attached cells developed the HMW DNA fragments after the drug-free interval, whereas MCF-7 cells did so only to a small extent (Fig. 5).

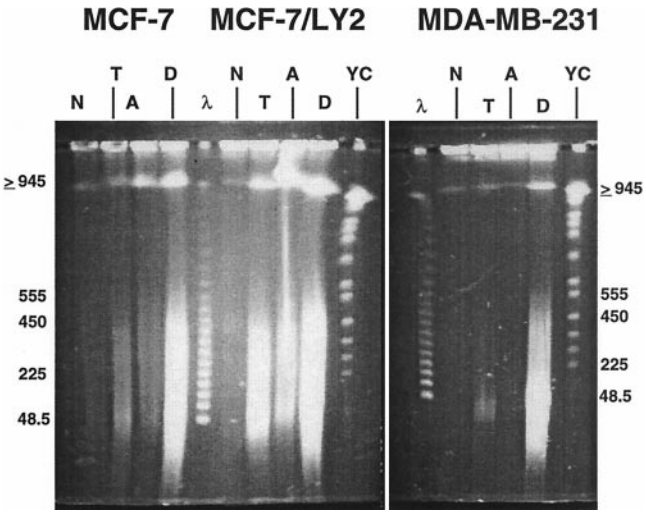

FIG. 4. Dependence of growth matrix-adherence status on the HMW DNA fragments formed in MCF-7, MCF-7/LY2, and MDA-MB-231 cells treated for 24 hr with 100 μM A_{II} detected by pulsed field gel electrophoresis on a 1.5% agarose gel. (N) total cells after growth in the presence of vehicle only; (T) total cells after drug treatment; (A) attached cells after drug treatment; (D) detached cells after drug treatment; (λ) lambda phage markers; (YC) *S. cerevisiae* chromosomes.

Single-color flow cytometric analysis showed that in all three cell lines any hypodiploid populations observed arose mainly or solely from detached cells. Other than the differences in hypodiploid cell numbers, there was no evidence to suggest any differences in cell cycle distribution between the adherent and detached cells of treated cultures (data not shown).

Effects on Other Human Breast Cell Lines

MCF-7 and MDA-MB-231 cells showed little to no accumulation of hypodiploid cells by PI flow cytometry. However, since by Hoechst staining and PFGE it was apparent that apoptosis was occurring in these cells, either their hypodiploid cells did not persist long enough to be visualized by single-color PI flow cytometry, or they were more sensitive to the preparative procedures we utilized (i.e. lysed during fixation). MCF-7/LY2 cells, however, did yield a convincing hypodiploid peak in response to A_{II}. Thus, we examined three additional human breast carcinoma cell lines to determine if we could observe a "usual" single-color flow pattern in them after treatment with A_{II}. The retinoic acid resistant/ER negative BT-20 line [33–35], the ER positive/estrogen-dependent CAMA-1 line [36, 37], and the metastatic/retinoic acid sensitive/ER negative SKBR-3 line [33, 34, 38] were examined in cell counting and PI flow cytometry experiments. The drug caused a rapid decrease in cell numbers of all three lines (Fig. 6, A–C). A_{II}-treated BT-20 cells showed stimulation into S phase and a dramatic increase in the hypodiploid cell population. Drug-induced G_2/M accumulation was apparent at 12 and 18 hr of treatment, which was followed by a loss of these cells at 24 hr (Fig. 6A). CAMA-1 cells showed a rapid and large increase in hypodiploid cells in response to A_{II} and a complete loss of hyperploid cells (Fig. 6B). Simultaneously, these cells had a dramatic reduction in G_2/M cells, followed in the end by a near complete loss of this cell population. The SKBR-3 line exhibited a 2- to 6-fold increase in its hypodiploid population in response to A_{II}, some evidence

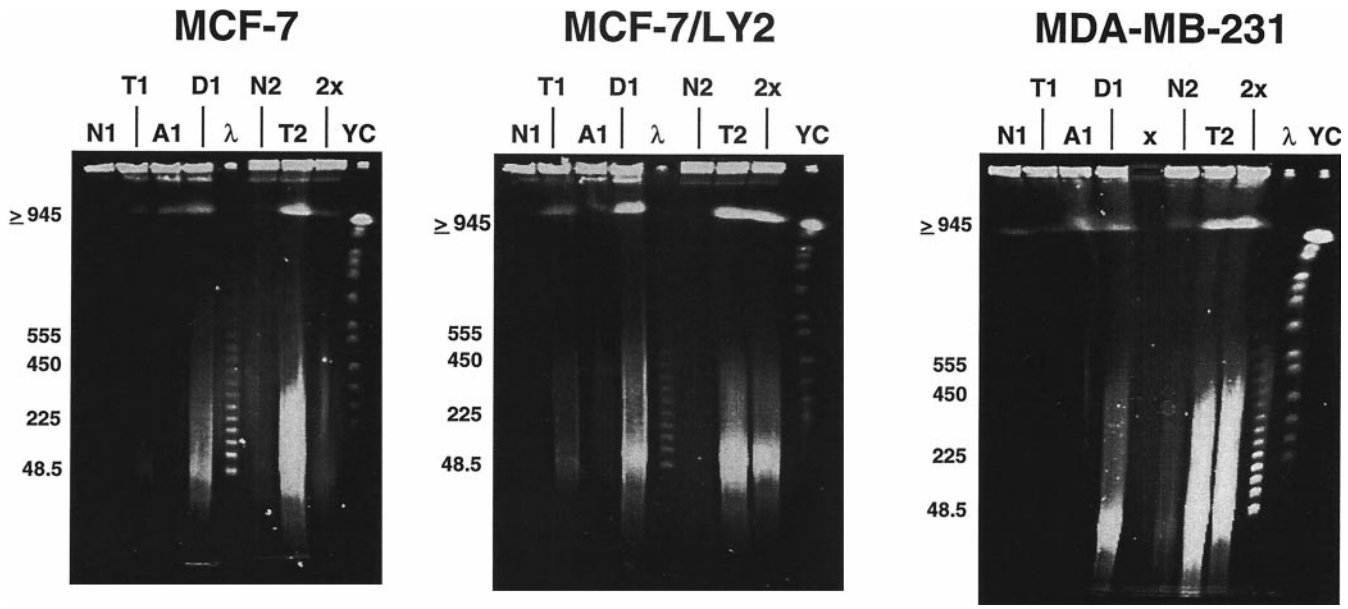

FIG. 5. Sustained HMW DNA fragment-inducing effects of A_{II}. Cells were treated with 100 μM drug for 24 hr, detached cells were removed, attached cells were grown in fresh, drug-free medium for an additional 24 hr, and all were analyzed by PFGE on a 1.5% agarose gel. (N1) total cells after 24 hr in the presence of vehicle only; (T1) total cells with 24-hr drug treatment; (A1) attached cells after 24 hr of drug; (D1) detached cells after 24 hr of drug; (N2) total cells after 48 hr in the presence of vehicle only; (T2) total cells after 48 hr of drug; (2x) total cells remaining after 24 hr of drug, detached cells removed, followed by remaining attached cells grown for 24 hr in the presence of vehicle only; (λ) lambda phage markers; (YC) *S. cerevisiae* chromosomes; and (x) empty lane.

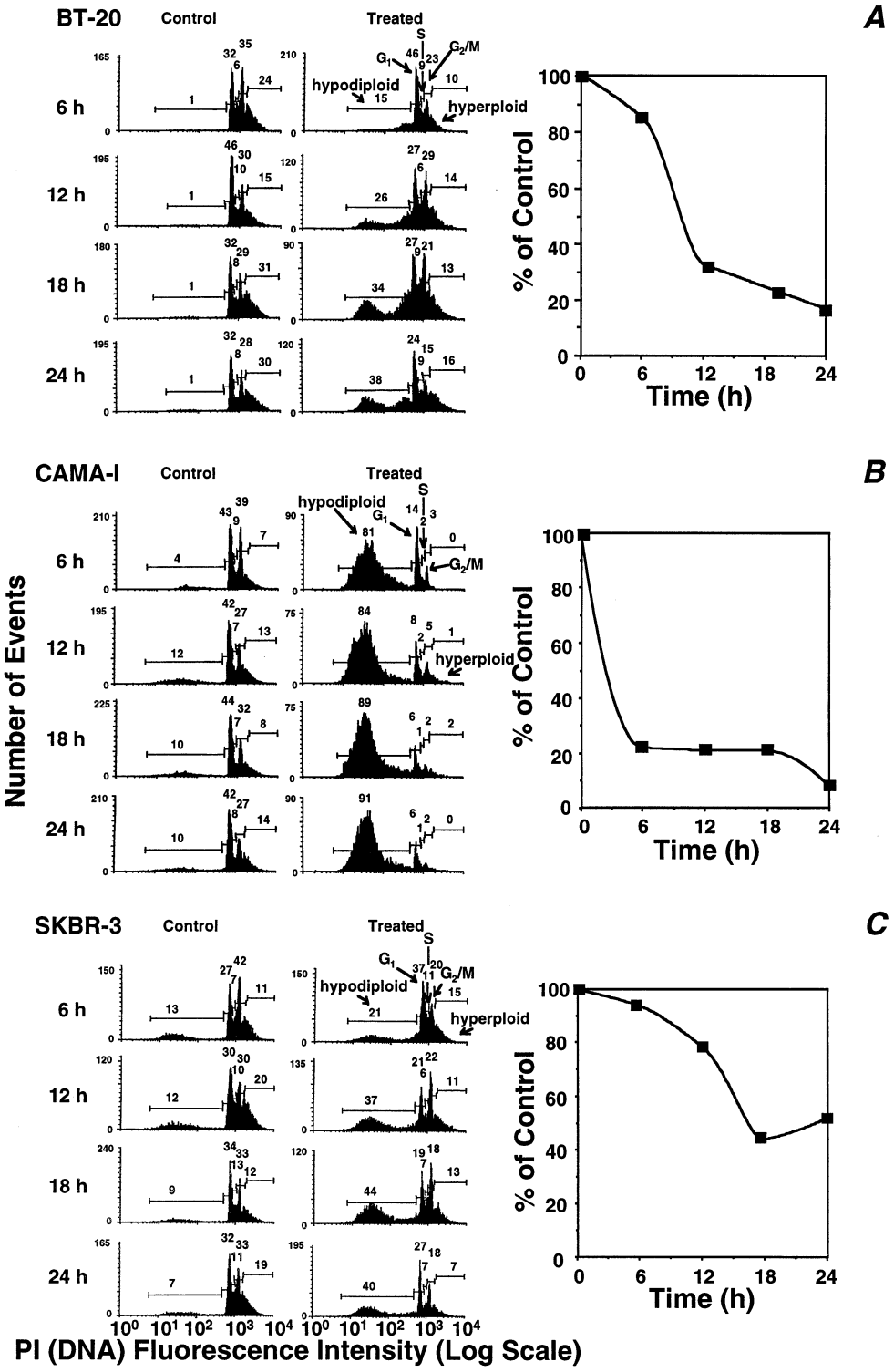

FIG. 6. Examples of PI flow cytometric and cell counting analyses of BT-20 (A), CAMA-1 (B), and SKBR-3 (C) human breast cancer cells treated with 100 μM A_{II} or vehicle for 6–24 hr. Attached cells were trypsinized, combined with floating cells, and Trypan blue-negative cells were quantified microscopically on a hemacytometer. Flow cytometric data were collected, quantified, and are displayed as in Fig. 3.

of stimulation into S phase, a transient G_2/M pileup followed by loss of G_2/M cells, and a decrease in hyperploid cells (Fig. 6C).

A non-tumorigenic, "normal" human breast cell line was also tested for its susceptibility to A_{II}. The MCF-10A line originated from spontaneous immortalization of breast epithelial cells obtained from a patient with fibrocystic disease, and is an ER negative line [39]. A_{II} at 100 μM had

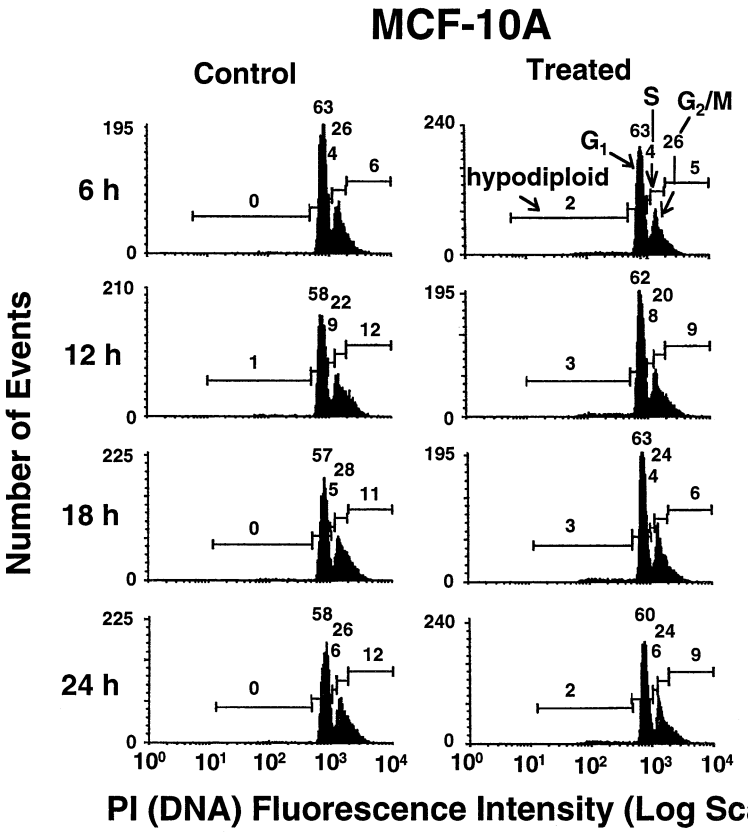

FIG. 7. Lack of effect of 100 μM A_{II} on the cell cycle distribution of MCF-10A cells. Data were collected, quantified, and are displayed as in Fig. 3.

no effect on the growth (data not shown) nor cell cycle distribution (Fig. 7) of this line.

Bromodeoxyuridine Labeling

Since some cell lines did show a hypodiploid peak (e.g. MCF-7/LY2 and CAMA-1) while others did not (e.g. MCF-7 and MDA-MB-231 cells), and some showed G_2/M accumulation and others gave the appearance of G_1 arrest, we performed BrdU labeling experiments to attempt to determine from which phase of the cell cycle A_{II} caused apoptosis and disappearance from flow analyses. The MCF-7, MCF-7/LY2, and MDA-MB-231 cell lines were treated under the same conditions as above in the presence of the pyrimidine base analogue BrdU. MCF-7/LY2 cells, which did show a hypodiploid peak, were also included to determine if apoptotic cells arose from the same portion of the cell cycle as did disappearing cells in the other two cell lines.

BrdU is incorporated into the DNA during S phase and can be visualized quantitatively with the addition of a monoclonal antibody labeled with a fluorescent reporter molecule, in this case fluorescein. As can be seen in the control cells shown in Fig. 8A–C, continuous growth in the presence of BrdU can define at least four distinct cell populations in a two-color flow cytometric analysis: cells unlabeled with BrdU with low or high PI staining corresponding to preexisting cells in G_1 and G_2/M, respectively, and the peaks evident in the single-color flow cytometric profiles. Incorporation of BrdU into newly synthesized DNA creates a smear of cells rising from the initial G_1 peak to a new G_2/M peak that has both a high PI signal and complete BrdU labeling. When these cells undergo mitosis, they create a final unique peak of BrdU-labeled G_1 cells directly above the original G_1 peak. Given a long enough experimental period, all of the unlabeled cells eventually enter S phase and become labeled with BrdU, leading to the disappearance of the unlabeled peaks: first the G_2/M peak, as those cells undergo mitosis to become unlabeled G_1 cells, then the G_1 cells as the entire supply of unlabeled cells in G_1 and G_2/M is exhausted. A poptotic (hypodiploid) cells appear to the left of G_1 cells, with low or high y-values if they have not or have, respectively, incorporated BrdU.

As shown in Fig. 8A–C, all three cell lines incorporated BrdU and exhibited the described cell populations in the course of a 24-hr exposure period, with minor differences in the timing of appearance of labeled cell populations. In the presence of A_{II} (Fig. 8D–F), all three cell lines incorporated BrdU more quickly than, but never to the same extent as, controls, and never formed a G_2/M peak as densely labeled as controls, indicative of a common cell cycle block and/or loss from the analysis at mitosis (although there were more subtle indications of further cell cycle blocks or changes in MCF-7 and MCF-7/LY2).

Drug-free MCF-7 cells accumulated in BrdU-labeled G_1 at 18 and 24 hr. A_{II}-treated MCF-7 cells showed a transient and early labeled G_1 peak at 6 and 12 hr that went

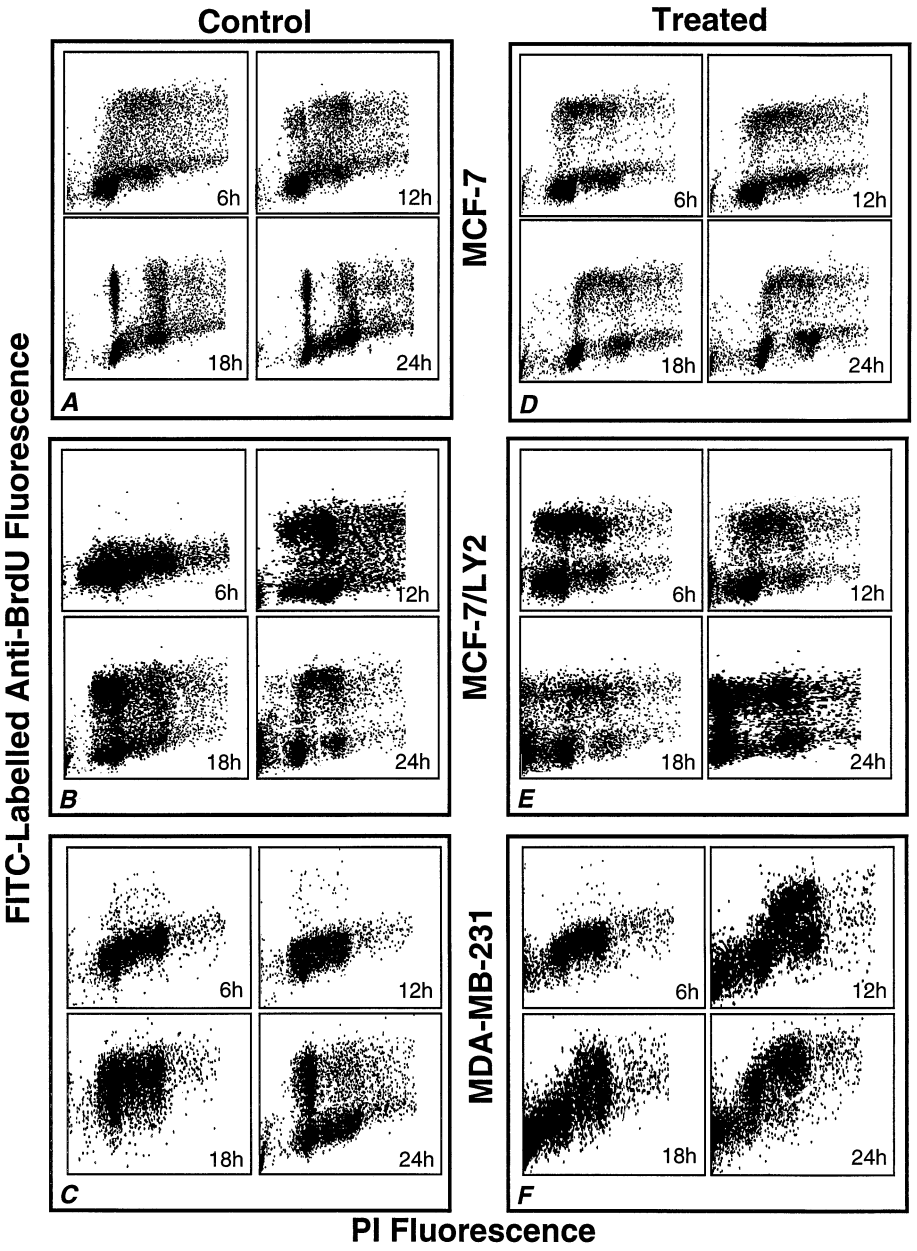

FIG. 8. Two-color flow cytometric analysis of DNA content (PI) and BrdU incorporation into newly synthesized DNA (fluorescein-labeled antibody to BrdU) of MCF-7 (A and D), MCF-7/LY2 (B and E), and MDA-MB-231 cells (C and F). Vehicle-treated control cells (A–C) and cells treated with 100 μM A_{II} (D–F). Data are presented with a linear x-axis and a log-scale y-axis.

away—these cells disappeared after S-phase labeling, i.e. death/disappearance from the analysis occurred from G_2/M and no BrdU-labeled apoptotic cells appeared. Untreated MCF-7/LY2 cells showed the expected, full pattern of BrdU labeling—labeled G_1 accumulation was evident at 18 hr. A_{II}-treated MCF-7/LY2 cells showed an initial stimulation into BrdU-labeled G_2/M and G_1. Cells in the initial apoptotic peak (12 hr) were all unlabeled. By 18 and 24 hr, significant apoptotic populations arose from both unlabeled and, with time, labeled cells. The unlabeled G_1 population was gone by 24 hr, and hypodiploid cells arose largely from labeled G_2/M. A_{II}-free MDA-MB231 cells showed one pulse of growth with a late, transient, BrdU-labeled G_2/M peak at 18 hr, followed by accumulation into labeled G_1. MDA-MB-231 cells treated with A_{II} showed a relatively early stimulation into BrdU-labeled G_2/M (12 hr instead of the 18 hr in control cells). All apoptotic cells were unlabeled throughout. This, coupled with the definite loss of unlabeled G_2/M peak shows that death occurred from G_2/M. The G_1 peak was smeared between definitely unlabeled and labeled cells, so the unlabeled G_2/M cells all either cycled to unlabeled G_1 or disappeared (= died). There was no evidence of labeled G_1 cells, so cells disappearing from analyses arose from both labeled G_2/M and unlabeled G_2/M.

Thus, only MCF-7/LY2 showed any evidence of labeled

TABLE 1. Protection by CHX against A_{II}-induced cell death

Cell line and treatment	% of Control cells†	*P* value*	% Rescue
MCF-7			
A_{II} (4 hr)			
CHX (12 hr) + A_{II} (4 hr)	78 ± 6	0.15	42
A_{II} (12 hr)	50 ± 4		
CHX (12 hr) + A_{II} (12 hr)	81 ± 4	< 0.001	61
MCF-7/LY2			
A_{II} (4 hr)	64 ± 4		
CHX (12 hr) + A_{II} (4 hr)	80 ± 3	0.004	44
A_{II} (12 hr)	41 ± 4		
CHX (12 hr) + A_{II} (12 hr)	78 ± 3	< 0.001	63
MDA-MB-231			
A_{II} (4 hr)	44 ± 7		
CHX (12 hr) + A_{II} (4 hr)	81 ± 6	0.002	67
A_{II} (12 hr)	31 ± 4		
CHX (12 hr) + A_{II} (12 hr)	82 ± 2	< 0.001	74

Samples (5×10^4 cells/well; N = 3) were preincubated with 18 μM CHX, washed with HBSS, then exposed to 100 μM A_{II} alone or in the presence of 18 μg/mL of CHX.

* Student's *t*-test.

† Mean ± SD.

apoptotic cells, and these may have been from initial cell cycle stimulation (prior to apoptotic effects), all consistent with apoptosis from G_2/M; furthermore, no BrdU-labeled G_1 cells appeared in the analyses of MCF-7 and MDA-MB-231 cells treated with A_{II}, showing that disappearing cells (and these are apoptotic based on our morphological and DNA digestion assays) arose from G_2/M.

Protection by CHX

The role of *de novo* protein synthesis in A_{II}-dependent apoptosis was also tested. Apoptosis in other transformed epithelial cells has been shown previously to often be dependent on the synthesis of new proteins [10], including perhaps the endonucleases responsible for HMW and internucleosomal DNA fragmentation, as has the action of microtubule-perturbing drugs [40]. Cells were treated with the maximum concentration of CHX that had no effect on cell viability but that blocked protein synthesis (by *ca.* 80%) for 12 hr, rinsed with fresh medium, and then were treated with A_{II} in both the absence and the presence of CHX. The cultures were incubated for an additional 4 and 12 hr, and cell numbers were determined at each time point. CHX significantly increased the survival of A_{II}-treated cells (Table 1), although at the concentration used it could not protect against about 20% of the death caused by A_{II}. This protection by CHX was also reflected in PFGE analyses, where reduced HMW DNA fragmentation was noted (data not shown). Furthermore, flow cytometric analysis showed that CHX alone had no effect on cell cycle distributions, while it protected against the cell cycle changes induced by A_{II} (data not shown). The protective effects of CHX are consistent with the hypothesis that A_{II}-induced cell cycle block, HMW DNA fragmentation, and cell death are, at least in part, translation-dependent processes.

DISCUSSION

A_{II}, an agent with direct effects on tubulin, antiestrogenic and antitumor properties in rodents, and cytostatic but no mutagenic properties *in vitro*, was investigated for its apoptosis-inducing effects against six different human breast cancer cell lines and a non-tumorigenic line. Our previous studies have shown that A_{II} and its major metabolite, Z-α-chlorochalcone, exert varying levels of cytotoxicity and cytostasis against the three cell lines analyzed initially in this study, MCF-7, MCF-7/LY2, and MDA-MB231 [6], and that both drugs disrupt cellular microtubule arrays [8]. The current experiments using the same cells showed that the cytostatic activity of A_{II} is associated with death from and/or block in G_2/M, nuclear fragmentation, detachment from the growth/extracellular matrix, *de novo* protein synthesis, and DNA digestion progressing to 30–50 kb fragments. Further studies with three additional breast carcinoma lines, BT-20, CAMA-1, and SKBR-3, verified the antiproliferative, G_2/M blocking and/or apoptosis-inducing effects of the compound. Like other microtubule-perturbing agents, A_{II} induced apoptosis in the carcinoma cells regardless of their p53 status [41]. Even at the high concentration used, however, A_{II} showed none of these actions against a "normal," non-tumorigenic human breast epithelial cell line, MCF-10A.

This observation of rapid cleavage of DNA into HMW fragments following exposure to A_{II} parallels findings that a number of neoplastic cells of epithelial origin (including breast cancer cells) respond to serum-starvation by undergoing HMW DNA fragmentation [9]. We saw no evidence of internucleosomal fragmentation (low molecular weight DNA fragments) in response to A_{II}. Observation of several other indices of apoptosis, including morphological and ploidal, also suggested that the drug was inducing programmed cell death. Based on experiments where the attachment status of cells was monitored, the results suggest that the mechanism by which A_{II} induces apoptosis in these breast cancer epithelial cells includes sequelae from loss of cellular contact with the growth matrix and/or loss of cell-to-cell contact or communication. Furthermore, it is apparent that apoptosis may be executed by breast cancer cells, at least in the three lines studied here by electrophoretic methods, through biochemical pathways that do not necessarily include internucleosomal fragmentation.

By flow cytometry, there was evidence of initial cell cycle stimulation by A_{II} in MCF-7, MCF-7/LY2, BT-20, and SKBR-3 cells. In the BrdU incorporation studies, this stimulation was further exemplified by earlier appearance of

labeled G_2/M MCF-7 cells, and of S phase and labeled G_2/M MCF-7/LY2 cells. In both cases, however, the dense accumulation of cells in the labeled G_1 phase seen in the controls was not apparent in the treated populations, indicating that after their initial cell cycle stimulation these cell lines experienced a drug-induced effect, cell cycle block, and death with or without the appearance of a hypodiploid population at mitosis. The stimulation of most of the cell lines by A_{II} into S phase is reminiscent of that induced by a structurally related compound, 1,1,1-trichloro-2,2-*bis*(chlorophenyl)ethane (DDT). DDT has been shown recently to stimulate Cdk2 activity, to cause hyperphosphorylation of pRB105, and to increase the synthesis of cyclin D, all apparently mediated by the ER [42]. There are several very important differences between the actions of A_{II} and DDT, however. One is that DDT is an estrogen agonist, whereas A_{II} has shown only estrogen antagonist actions. Moreover, A_{II} very quickly induces breast carcinoma cells to die, whereas DDT does not [43]. The concentration of A_{II} used in this study was certainly high enough for it to compete with estradiol for the ER (i.e. for rat uterine ER, 20 μM A_{II} would compete away *ca.* 50% of 2 nM estradiol [4]). Since we observed induction into S phase, G_2/M block, and apoptosis in both ER positive and ER negative cell lines, however, any potential participation of the ER in the effects of A_{II} appears to be a moot point.

The BrdU-labeled G_1 peak never appeared in the A_{II}-treated MDA-MB-231 cell population, also indicative of an inability to undergo mitosis. This is sufficient to explain the increased G_2/M peak observed in this and our earlier study [8] with MDA-MB-231. Another unique feature of the MDA-MB-231 analysis was the complete disappearance of the unlabeled G_2/M peak. If these cells could not undergo mitosis, they must have been dying, perhaps through a mechanism that produced the observed slight rise in hypodiploid cells. We do not know if or to what degree the hypodiploid populations observed were dynamic, i.e. although the hypodiploid population of MDA-MB-231 cells never became large, hypodiploidy might have been a fairly transient state prior to complete chromatin digestion—therefore, it should not be expected that the quantitative size of the hypodiploid peak necessarily shows good correspondence with the input "missing" cells, in this case the unlabeled G_2/M peak.

Like those seen in the control cultures of BrdU experiments, the slightly higher populations of hypodiploid cells observed in the treated MCF-7 and MDA-MB-231 cells were unlabeled. Therefore, either they did not traverse S phase, i.e. replicate their DNA in the presence of the drug prior to apoptosing, or they disappeared from the analysis as they apoptosed. The relatively small increases in apoptotic cells observed in these experiments may be indicative of a separation of purely cytostatic effects from cytotoxic effects, or may indicate a rapid traversal of the hypodiploid state before being lost to the analysis. The large hypodiploid peak induced by A_{II} in the MCF-7/LY2 line also consisted, in part, of unlabeled cells; however, there was a transient appearance of labeled apoptotic cells at 18 hr that was gone at 24 hr (giving some idea of the persistence of hypodiploid cells, in general). We suggest that the unlabeled hypodiploid MCF-7/LY2 cells consisted of those that were initially stimulated into the S phase upon A_{II} treatment, prior to any cell cycle blocks. These cells, therefore, likely arose from G_2/M, and definitely apoptosed through a mechanism involving hypodiploidy, apoptotic bodies, and HMW DNA fragmentation.

The absence of obvious G_2/M accumulation in MCF-7 and CAMA-1 cells suggests that they may have experienced a G_1 block as well, or that G_2/M cells died instead of accumulating. We assume that the latter is true and that A_{II} must have affected its actions in MCF-7 cells in a manner that did not proceed through the production of stable hypodiploid cells, since this population increased only slightly in response to the drug, whereas hypodiploid cells were abundant in CAMA-1 cells. Despite evidence for a mitotic block in response to A_{II} in MCF-7/LY2 cells, there was a paradoxical significant increase in the G_1 to G_2/M ratio. The differences seen in the MCF-7 and, for example, the MDA-MB-231 cells could be indicative of their differing p53 status and the ability of MCF-7 to induce p21 (WAF1/CIP1) expression that led to transient G_1 arrest [44, 45]. A more efficient G_1 block might also explain this observation. It is more likely that a greater loss from the G_2/M population occurred, which in the case of the CAMA-1 cells contributed to the large hypodiploid population, and in the case of the MCF-7 cells led to a loss of cells from the flow cytometric analyses. The transient nature of G_2/M accumulation followed by the loss of G_2/M cells in BT-20 and SKBR-3, coupled with the appearance of a hypodiploid population in these cells and the following disappearance of the G_2/M population, further argues that the mechanism of the drug includes effects at mitosis, followed more or less rapidly, depending on the cell line examined, by death of cells from G_2/M. We conclude, therefore, that A_{II} causes effects at G_2/M that lead to rapid apoptosis, which, in some cell lines, is difficult to observe solely by flow cytometry.

At the concentration used in this study, A_{II} causes microscopically discernable disruption of the cellular microtubule network within 1 hr of treatment [8]. The current results are comparable with studies on drugs that act on microtubule structure and function. For example, cells treated with the microtubule-stabilizing agents paclitaxel and discodermolide experience G_2/M arrest and undergo HMW DNA fragmentation before undergoing apoptosis [27, 32, 46]. In the present experiments, G_2/M arrest led to rapid nuclear fragmentation and, especially in the case of MCF-7/LY2, BT-20, CAMA-1, and SKBR-3 cells, the appearance of hypodiploid cells. The MDA-MB-231, BT-20, and SKBR-3 cells showed obvious G_2/M phase arrest. Although cell cycle arrest following cellular/DNA damage generally occurs at the G_1 or G_2 stage of the cell cycle, cell lines have been shown to enter apoptosis from all stages of the cell cycle [23]. Based on previous and the current

results, we envision the following scheme in the initiation of apoptosis in epithelial breast cancer cells by A_{II}:

Microtubule perturbation → Stimulation of interphase cells (increased S phase) → Cell cycle arrest in G_2/M → Nuclease synthesis → Nuclear fragmentation → Extracellular matrix nonadherence → DNA fragmentation (30–50 kb) → Cell death.

Based on the differences seen in flow cytometric experiments, we must also conclude that the rates of the above steps are cell line dependent.

The HMW DNA fragmentation detected with A_{II} coincides with cellular changes that have been linked in other cell types to internucleosomal fragmentation. A_{II}-treated cells become nonadherent in a time-dependent manner, indicating that changes in the extracellular matrix are associated with DNA fragmentation. This observation is consistent with the finding that DNA fragmentation occurs in some epithelial cells after detachment from the basement membrane, but can be blocked by bcl-2 overexpression [17]. Since the A_{II}-induced effects were largely blocked by CHX, the necessity of *de novo* protein synthesis indicates that cells respond to the drug by synthesizing new proteins, one of them likely the nuclease that cleaves chromatin to the observed 30–50 kb HMW DNA fragments, as well as others that may be involved in mitotic events, including detachment from the growth matrix.

In summary, the data obtained indicate that A_{II} may be a valuable agent for breast cancer chemotherapy, as well as for the study of apoptosis in various cancer cell lines of epithelial origin. The low toxicity and nongenotoxic nature of the drug further strengthen its attractiveness as a potential antitumor agent.

This work was supported, in part, by grants to B.W.D. from the National Cancer Institute (CA 57288), the University of Pittsburgh Cancer Institute Breast Cancer Initiative and the University of Pittsburgh Central Development Research Fund, and to S.G.G. from the American Cancer Society (IRG-58-35). E.tH. was supported, in part, by a Predoctoral Fellowship as part of a grant from the WM Keck Foundation for Advanced Training in Computational Biology at the University of Pittsburgh, Carnegie Mellon University, and the Pittsburgh Supercomputing Center. We thank Dr. Marc Lippman for the early passage MCF-7 cells and MCF-7/LY2 cells, and Profs. Robert E. Ferrell and Charles W. Richard III for use of their PFGE equipment and the assistance of their staffs with it.

References

1. Pento JT, Magarian RA and King MM, A comparison of the efficacy for antitumor activity of the non-steroidal antiestrogens Analog II and tamoxifen in DMBA-induced rat mammary tumors. *Cancer Lett* **15:** 261–269, 1982.
2. King MM, Pento JT, Magarian RA and Brueggemann GL, The interaction of dietary fat and antiestrogen treatment on DMBA-induced mammary tumors in the rat. *Nutr Cancer* **7:** 239–249, 1985.
3. King MM, Magarian RA, Terao J and Brueggemann GL, Effects of nonsteroidal antiestrogens, analog II and tamoxifen, on a metastatic transplantable rat mammary tumor. *J Natl Cancer Inst* **74:** 447–451, 1985.
4. Day BW, Magarian RA, Pento JT, Jain PT, Mousissian GK and Meyer KL, Synthesis and biological evaluation of 1,1-dichloro-2,2,3-triarylcyclopropanes as pure antiestrogens. *J Med Chem* **34:** 842–851, 1991.
5. Pento JT, Magarian RA, Wright RJ, King MM and Benjamin EJ, Non-steroidal estrogens and antiestrogens. Biological activity of cyclopropyl analogs of stilbene and stilbenediol. *J Pharm Sci* **70:** 339–343, 1981.
6. ter Haar E and Day BW, Cytostatic and cytotoxic action of *Z*-1,1-dichloro-2,3-diphenylcyclopropane in three human breast cancer cell lines. *Anticancer Res* **16:** 1107–1115, 1996.
7. Rajah TT and Pento JT, The mutagenic potential of antiestrogens at the HPRT locus in V79 cells. *Res Commun Mol Pathol Pharmacol* **89:** 85–92, 1995.
8. ter Haar E, Hamel E, Balachandran R and Day BW, Cellular targets of the anti-breast cancer agent *Z*-1,1-dichloro-2,3-diphenylcyclopropane: Type II estrogen binding sites and tubulin. *Anticancer Res* **17:** 1861–1870, 1997.
9. Dive C, Evans CA and Whetton AD, Induction of apoptosis—New targets for cancer chemotherapy. *Semin Cancer Biol* **3:** 417–427, 1992.
10. Kerr JFR, Winterford CM and Harmon BV, Apoptosis: Its significance in cancer and cancer therapy. *Cancer* **73:** 2013–2016, 1994.
11. Hickman JA, Apoptosis induced by anticancer drugs. *Cancer Metastasis Rev* **11:** 121–139, 1992.
12. Cotter TG, Glynn JM, Echeverri F and Green DR, The induction of apoptosis by chemotherapeutic agents occurs in all phases of the cell cycle. *Anticancer Res* **12:** 773–780, 1992.
13. Dive C and Hickman JA, Drug target interactions: Only the first step in the commitment to a programmed cell death. *Br J Cancer* **64:** 192–196, 1992.
14. Martin SJ, Apoptosis: Suicide, execution or murder? *Trends Cell Biol* **3:** 141–144, 1993.
15. Martin SJ, Green DR and Cotter TG, Dicing with death: Dissecting the components of the apoptosis machinery. *Trends Biochem Sci* **19:** 26–30, 1994.
16. Compton MM, A biochemical hallmark of apoptosis: Internucleosomal degradation of the genome. *Cancer Metastasis Rev* **11:** 105–109, 1992.
17. Frisch SM and Francis H, Disruption of epithelial cell-matrix interactions induces apoptosis. *J Cell Biol* **124:** 619–626, 1994.
18. Oberhammer F, Wilson JW, Dive C, Morris ID, Hickman JA, Wakeling AE, Walker PR and Sikorska M, Apoptotic death in epithelial cells: Cleavage of DNA to 300 and/or 50 kb fragments prior to or in the absence of internucleosomal fragmentation. *EMBO J* **12:** 3679–3684, 1993.
19. Rusnak JM, Calmels TPG, Hoyt DG, Kondo Y, Yalowich JC and Lazo JS, Genesis of discrete high order DNA fragments in apoptotic human prostate carcinoma cells. *Mol Pharmacol* **49:** 244–252, 1996.
20. Walker PR, Kokileva L, Le Blanc J and Sikorska M, Detection of the initial stages of DNA fragmentation in apoptosis. *Biotechniques* **15:** 105–109, 1993.
21. Brown DG, Sur XM and Cohen GM, Dexamethasone-induced apoptosis involves cleavage of DNA to large fragments prior to internucleosomal fragmentation. *J Biol Chem* **268:** 3037–3039, 1993.
22. Huang P, Ballal K and Plunkett W, Biochemical characterization of the protein activity responsible for high molecular weight DNA fragmentation during drug-induced apoptosis. *Cancer Res* **57:** 3407–3414, 1997.
23. Fan S, Smith ML, Rivet DJ II, Duba D, Zhan Q, Kohn KW and Fornace AJ Jr, Disruption of p53 function sensitizes breast cancer MCF-7 cells to cisplatin and pentoxifylline. *Cancer Res* **55:** 1649–1654, 1995.
24. Kyprianou N, English HF, Davidson NE and Isaacs JT,

Programmed cell death during regression of the MCF-7 human breast cancer following estrogen ablation. *Cancer Res* **51:** 162–166, 1991.
25. Armstrong DK, Kaufmann SH, Ottaviano YL, Furuya Y, Buckley JA, Isaacs JT and Davidson NE, Epidermal growth factor-mediated apoptosis of MDA-MB-468 human breast cancer cells. *Cancer Res* **54:** 5280–5283, 1994.
26. Armstrong DK, Isaacs JT, Ottaviano YL and Davidson NE, Programmed cell death in an estrogen-independent human breast cancer cell line, MDA-MB-468. *Cancer Res* **52:** 3418–3424, 1992.
27. McCloskey DE, Kaufmann SH, Prestigiacomo LJ and Davidson NE, Paclitaxel induces programmed cell death in MDA-MB-468 human breast cancer cells. *Clin Cancer Res* **2:** 847–854, 1996.
28. Magarian RA and Benjamin EJ, Syntheses of cyclopropyl analogs of stilbene and stilbenediol as possible antiestrogens. *J Pharm Sci* **64:** 1626–1632, 1975.
29. Jonnalagadda SS, ter Haar E, Hamel E, Lin C, Magarian RA and Day BW, Synthesis and biological evaluation of 1,1-dichloro-2,3-diarylcyclopropanes as antitubulin and anti-breast cancer agents. *Bioorg Med Chem* **5:** 715–722, 1997.
30. Dolbeare F, Gratzner HG, Pallavicini MG and Gray JW, Flow cytometric measurement of total DNA content and incorporated bromodeoxyuridine. *Proc Natl Acad Sci USA* **80:** 5573–5577, 1983.
31. Hamel E, Antimitotic agents and their interactions with tubulin. *Med Res Rev* **16:** 207–231, 1996.
32. Balachandran R, ter Haar E, Welsh MJ, Grant SG and Day BW, The microtubule-stabilizing agent (+)-discodermolide induces apoptosis in human breast carcinoma cells—Preliminary comparisons to paclitaxel. *Anticancer Drugs* **9:** 67–76, 1998 [erratum pp. 369–370].
33. Widschwendter M, Daxenbichler G, Dapunt O and Marth C, Effects of retinoic acid and γ-interferon on expression of retinoic acid receptor and cellular retinoic acid-binding protein in breast cancer cells. *Cancer Res* **55:** 2135–2139, 1995.
34. Widschwendter M, Daxenbichler G, Culig Z, Michel S, Zeimet AG, Mörtl MG, Widschwendter A and Marth C, Activity of retinoic acid receptor-γ selectively binding retinoids alone and in combination with interferon-γ in breast cancer cell lines. *Int J Cancer* **71:** 497–504, 1997.
35. Betz NA, Fattaey HK, Westhoff BA, Paulsen AQ and Johnson TC, CeReS-18, a novel cell surface sialoglycopeptide, induces cell cycle arrest and apoptosis in a calcium-sensitive manner. *Breast Cancer Res Treat* **42:** 137–148, 1997.
36. Ji HJ, Zhang QQ and Leung BS, Survey of oncogene and growth factor/receptor gene expression in cancer cells by intron-differential RNA/PCR. *Biochem Biophys Res Commun* **170:** 569–575, 1990.
37. Yu WC, Leung BS and Gao YL, Effects of 17β-estradiol on progesterone receptors and the uptake of thymidine in human breast cancer cell line CAMA-1. *Cancer Res* **41:** 5004–5009, 1981.
38. Turley JM, Fu T, Ruscetti FW, Mikovits JA, Bertolette DC 3rd and Birchenall-Roberts MC, Vitamin E succinate induces Fas-mediated apoptosis in estrogen receptor-negative human breast cancer cells. *Cancer Res* **57:** 881–890, 1997.
39. Soule HD, Maloney TM, Wolman SR, Peterson WD Jr, Brenz R, McGrath CM, Russo J, Pauley RJ, Jones RF and Brooks SC, Isolation and characterization of a spontaneously immortalized human breast epithelial cell line, MCF-10. *Cancer Res* **50:** 6075–6086, 1990.
40. Liebman J, Cook JA, Teague D, Fisher J and Mitchell JB, Cycloheximide inhibits the cytotoxicity of paclitaxel (Taxol). *Anticancer Drugs* **5:** 287–292, 1994.
41. Blagosklonny MV and El-Deiry WS, Acute overexpression of wt p53 facilitates anticancer drug-induced death of cancer and normal cells. *Int J Cancer* **75:** 933–940, 1998.
42. Dees C, Askari M, Foster JS, Ahamed S and Wimalasena J, DDT mimicks estradiol stimulation of breast cancer cells to enter the cell cycle. *Mol Carcinog* **18:** 107–114, 1997.
43. Zava DT, Blen MA and Duwe G, Estrogenic activity of natural and synthetic estrogens in human breast cancer cells in culture. *Environ Health Perspect* **105** (Suppl 3): 637–645, 1997.
44. Tishler RB and Lamppu DM, The interaction of taxol and vinblastine with radiation induction of p53 and p21 WAF1/CIP1. *Br J Cancer* **74** (Suppl 27): S82–S85, 1996.
45. Khan SH and Wahl GM, p53 and pRb prevent rereplication in response to microtubule inhibitors by mediating a reversible G_1 arrest. *Cancer Res* **58:** 396–401, 1998.
46. Balachandran R, Grant SG, Welsh MJ and Day BW, Increased sensitivity of the antiestrogen-resistant MCF-7/LY2 human breast carcinoma cell line to apoptosis induced by the novel microtubule-stabilizing agent (+)-discodermolide. *Breast J* **4**: in press, 1998.